science, engineering and health studies

Research Article

*Science, Engineering and Health Studies*
*https://lio1.tci-thaijo.org/index.php/sehs*
*ISSN (Online): 2630-0087*

# Effect of aluminum hybrid additive on water absorption of fiber-cement composites

*Juthamat Nithipaiboon[1], Wichit Prakaypan[2], Parinya Chakartnarodom[3], Edward A Laitila[4], and Nuntaporn Kongkajun[1,5*]*

[1] Department of Materials and Textile Technology, Faculty of Science and Technology, Thammasat University, Pathum Thani 12121, Thailand
[2] Source Runner Enterprises Company Limited, Bang Khen, Bangkok 10220, Thailand
[3] Department of Materials Engineering, Faculty of Engineering, Kasetsart University, Bangkok 10900, Thailand
[4] Department of Materials Science and Engineering, Michigan Technological University, Houghton, MI 49931, USA
[5] Thammasat University Research Unit in Sustainable Materials and Circular Economy, Thammasat University, Pathum Thani 12121, Thailand

## ABSTRACT

Moisture movement and aggressive ions being transferred into a fiber-reinforced cement composite structure have negative effects in terms of mechanical properties and durability. When an aluminum hybrid additive (AHA) is incorporated into a fiber-reinforced cement composite composition, its reaction product provides a water-repellent layer along the capillary pores, resulting in a damp-proofing effect. In this study, the influences of AHA on the hydration reaction kinetics and microstructural features were characterized by isothermal calorimetry and thermogravimetry analysis. The percentages of AHA added to the mixtures varied from 0 to 5% w/w. The samples were formed by a filter-pressing process. After the sample forming process, the green samples were cured in air for 7, 14 and 28 days. The addition of 3% w/w AHA, based on the weight percent of cement, shortened the setting time of cement paste by almost 40%. Microstructural analysis of the cement matrix showed packing efficiency of the crystalline phase was improved when adding 3% w/w AHA to the mixture. This AHA mixture showed integral hydrophobicity, with contact angles greater than 140° on the surface and 16.51% porosity. These results corresponded to a decrease in water absorption of almost 50%, compared to the reference composition. Moreover, the enhancement of the mechanical properties of the samples, including modulus of elasticity, modulus of rupture and impact strength, surpassed the requirements for wallboard applications.

**Keywords:** fiber-cement composites; water absorption; additive; aluminum

***Corresponding author**:
Nuntaporn Kongkajun
n-kongkj@tu.ac.th

***Received***: *17August 2023*
***Revised***: *5 November 2023*
***Accepted***: *15 November 2023*
***Published***: *31 December 2023*

***Citation***:
*Nithipaiboon, J., Prakaypan, W., Chakartnarodom, P., Laitila, E. A., and Kongkajun, N. (2023). Effect of aluminum hybrid additive on water absorption of fiber-cement composites. Science, Engineering and Health Studies, 17, 23040013.*

## 1. INTRODUCTION

Fiber-cement products typically comprise fiber-reinforced building materials with cement as the matrix. These composites are found extensively in various building components such as flooring, roofing, and walls due to beneficial properties including low density, high flexural capacity, and cost-effectiveness. The fabrication of fiber-cement composites primarily requires raw materials such as cement, sand, fibers, and water. The mixture is prepared and then formed into green sheets using processes such as filter pressing and the

Hatschek process (Khorami and Ganjian, 2011; Mohr et al., 2005).

Water absorption is another important property of fiber-cement. The cement matrix and thus cement-based products generally have a high hydrophilicity due to their many pores. This porous structure causes greater permeability of water or diffusion of aggressive ions into the material. Water penetration causes deterioration of mechanical properties, corrosion resistance, and durability (Yao et al., 2021; Min and Song, 2018; Zheng et al., 2019; Azarsa et al., 2020). Thus, the reduction of water penetration into cement-based materials is beneficial. This can be accomplished by improving the compaction and by optimizing the water-to-cement ratio. However, this makes it more difficult to control the workability of the cement paste.

Currently, various methods are commonly employed to enhance the hydrophobicity of cement. One approach is to prevent contact between environmental water and the cement through surface hydrophobic post-treatments, which include methods such as coating, dipping, and spraying. Silane or siloxane-based surface treatments applied to the cement surface have shown improved hydrophobicity (Liu et al., 2016; Liu et al., 2017). Moreover, a silica-based hybrid nanocomposite has shown a lotus-leaf-like microstructure on the cement surface that enhances the water-repellent properties and refines the pore structure (Li et al., 2018). However, the coating surface can be mechanically destroyed during service, with the exposed cement surface becoming hydrophilic.

The second approach to limit water penetration in cementitious materials is by introducing nanoparticles into cement mixture. Some commonly used nanoparticles include nanosilica, nano-$TiO_2$, and nano-$CaCO_3$ (Faraj et al., 2022; Abdalla et al., 2022; Raabe et al., 2022). The incorporation of nanoparticles demonstrates improvements in the microstructure and mechanical properties of cement-based products. Previous work by Faraj et al. (2022) showed that adding nanosilica to cementitious materials enhanced the hydration reaction of cement with lower water requirements and gas permeability of the samples. A study of the replacement of Portland cement with nano-$CaCO_3$ and nano-$TiO_2$ showed that both nanoparticles used as a filler achieved a denser microstructure and refined the pore structure of the cement matrix (Abdalla et al., 2022). In addition, work by Raabe et al. (2022) on a modified nanosilica cellulose fiber surface found that nanosilica on surface fiber reduces water absorption and increases the hydrophilicity of composites.

An alternative approach known as internal hydrophobic modification involves adding a hydrophobic substance during the mixing of cement. This method results in cement that exhibits excellent hydrophobicity, not only in the bulk but also on the surface. In addition, increasing industrial waste generation on a global scale means there is a growing interest in using waste materials as additives for cement and construction applications. Industrial wastes, including paper sludge ash, rubber, and short textile waste fibers, have been the subject of investigation in this context (Wong et al., 2015; Chen et al., 2021; Sadrolodabaee et al., 2021).

In a study conducted by Wong et al. (2015), hydrophobic powders derived from paper sludge ash were examined. Their findings indicated that replacing 12% of Portland cement with paper sludge ash led to an 84% reduction in water absorption without negatively impacting material strength. Another investigation by Chen et al. (2021) explored the use of crumb rubber treated with partial oxidation as an additive in cement paste. The study revealed that pretreated crumb rubber facilitated the development of a hydrophobic rubberized cement paste. Additionally, Sadrolodabaee et al. (2021) employed short textile waste fibers containing polyester and cotton, sourced from textile industries, in cement composites. The research demonstrated that incorporating 8% of the cement weight of short textile waste fibers resulted in cement composites with optimal compressive and flexural strength.

Various hydrophobic substances have been incorporated into cement-based materials to enhance their water resistance. Examples of such substances include fatty acid, stearic acid, and paper sludge ash, as investigated by Lagazzo et al. (2016), Li et al. (2019), and Azarhomayun et al. (2022), respectively. Lagazzo et al. (2016) utilized fatty acids as a hydrophobic substance and observed improved waterproofing properties in mortars. Li et al. (2019) focused on modified Fenton paper sludge ash and reported an increase in mechanical strength, including bending and compressive strength, at the 28-day mark. Azarhomayun et al. (2022) studied the impact of calcium stearate and aluminum powder and demonstrated damp-proofing capabilities in cement-based materials. Additionally, Chen and Sun (2018) explored the use of an alkali-free accelerator produced from aluminum sulfate in cement, resulting in shortened setting times and the enhanced hydration degree and strength of the cement paste, attributed to the formation of a tightly meshed structure of the ettringite phase.

Currently, several types of industrial by-products, such as aluminum dross and flue gas desulfurized gypsum, are being incorporated into concrete production. Aluminum dross, which consists primarily of alumina, is from the aluminum melting process. Gas-desulfurized gypsum is from the desulfurization process of flue gas in coal-fired power plants. In concrete production, a study conducted by Mailar et al. (2016) found that the application of recycled aluminum dross resulted in concrete with greater mechanical and durability properties. Similarly, Pang et al. (2020) investigated the use of gas-desulfurized gypsum and ground granulated blast furnace slag in a cementitious material for mortar and found that the combined utilization of these waste materials led to improved mechanical properties in the resulting material.

A new approach to both achieve a hydrophobic surface and enhance the mechanical properties in fiber-cement by using an aluminum hybrid additive (AHA) blended with fresh cement paste has been proposed. This AHA is derived from aluminum dross and flue gas-desulfurized gypsum. The impacts of the AHA on the physical and mechanical properties of fiber-cement composites were investigated, including bulk density, water absorption, modulus of rupture, modulus of elasticity, and impact strength. Scanning electron microscopy (SEM) and mercury intrusion porosimetry (MIP) were employed to investigate the impact of the additive on the microstructure of the cement matrix. Furthermore, contact angle measurements were taken to assess the hydrophobicity of the materials.

## 2. MATERIALS AND METHODS

### 2.1 Materials

The fabrication of fiber-cement composite specimens involved the use of type I Portland cement (OPC), sand, and fibers which comprised polyvinyl alcohol (PVA) and cellulose fibers (Celco Cellulose Consulting). OPC was based on ASTM C150 and sand particles smaller than 75 microns in size. Gas-desulfurized gypsum, a waste product from the Mae Moh power plant, and aluminum dross, a byproduct from secondary aluminium production, were used to produce the additive. The chemical composition of the calcined aluminum dross and gas-desulfurized gypsum was monitored using X-ray fluorescence spectroscopy (Phillips PW2404). The summarized results are presented in Table 1.

**Table 1.** Chemical composition of aluminum dross and FGD gypsum as determined by X-ray fluorescence spectroscopy

| Substance | Chemical composition (% w/w) | | | | | | |
|---|---|---|---|---|---|---|---|
| | $SiO_2$ | $Al_2O_3$ | $SO_3$ | CaO | $Fe_2O_3$ | Others | LOI |
| **Calcined aluminum dross** | 15.56 | 65.6 | 1.95 | 7.76 | 3.33 | 5.80 | - |
| **FGD gypsum** | 0.14 | 0.15 | 73.07 | 24.56 | 0.10 | 1.98 | 22.01 |

### 2.2 Material preparation

The compositions of the dry mixtures were prepared based on the amounts listed in Table 2. The reference composition from Table 2, identified as REF, served as the control formula. Formula REF is commonly used in wallboard applications for fiber-cement composites. The AHA consisted of calcined aluminum dross and gas-desulfurized gypsum, maintaining an $Al^{3+}$:$SO_4^{2-}$ ratio of 1:1.5, as established in a previous study conducted by Nithipaiboon et al. (2023). The slurry was prepared by blending the dry mixture with water followed by shaping using the filter pressing method. To produce the slurry, a consistent water-to-cement ratio (w/c ratio) of 0.3 was maintained. Subsequently, the green samples were subjected to air curing for 7, 14, and 28 days.

**Table 2.** Formulation and identification of the various dry mixtures

| Formula | Raw materials (% w/w) | | | | |
|---|---|---|---|---|---|
| | OPC | Sand | Cellulose fibers | PVA fibers | AHA |
| REF | 70 | 25 | 4 | 1 | 0 |
| AHA1 | 69 | 25 | 4 | 1 | 1 |
| AHA2 | 68 | 25 | 4 | 1 | 2 |
| AHA3 | 67 | 25 | 4 | 1 | 3 |
| AHA4 | 66 | 25 | 4 | 1 | 4 |
| AHA5 | 65 | 25 | 4 | 1 | 5 |

### 2.3 Testing methods

#### 2.3.1 Phase determination and degree of hydration analysis

Phase analysis was accomplished using X-ray diffraction (XRD) (Phillips X' pert X-ray diffractometer). To obtain the hydration reaction data, the heat released during the hydration reaction of the slurry was analyzed following the guidelines outlined in ASTM C186 standards. Thermogravimetric analysis and derivative thermogravimetric analysis (TGA/DTG) were conducted at a heating rate of 10 °C/min using a NETZSCH STA 449 F5 thermal analyzer. The temperature ranged between 25 °C and 1,000 °C under a nitrogen atmosphere.

#### 2.3.2 Determination of physical properties of the samples

A universal testing machine was used to collect data to determine the mechanical properties of the modulus of rupture and modulus of elasticity, based on the ASTM C1185 standard. The test sample dimensions were 75 mm × 200 mm × 7 mm. The impact strength of the samples was determined by a pendulum impact testing machine. The bulk density and water absorption of the samples were determined using the Archimedes method. Ten specimens were used for each mechanical and physical property test. The microstructure of the specimens was observed by SEM using a JEOL JSM-64OLV. The pore structure of the samples was determined by MIP (Auto pore V, Micromeritics).

The hydrophobicity of materials can be determined by water wettability (contact angle), and the contact angle was used to determine the wetting behavior of water on a solid surface (hydrophilicity $\theta<90°$ or hydrophobicity $\theta>90°$). After 28 days curing, the samples were cut and sanded to obtain a smooth surface. The contact angles between the water droplets and the sample surface were determined at room temperature using a contact angle meter (Theta lite Optical tensiometer TL100).

## 3. RESULTS AND DISCUSSION

### 3.1 Impact of AHA on heat of hydration

The heat generated due to the exothermic reaction of the cement was observed by temperature collection of the heat evolution from the hydration reaction. Initially, the temperatures increased with time. The cement paste was hydrated when reaching a maximum temperature ($T_{max}$) at the setting time ($t_{set}$). The relationship between the

maximum temperature and setting time of cement paste versus AHA content is illustrated in Figure 1. Increasing the amount of AHA from 1 to 5% w/w of the dry mixture caused the setting time or time to reach maximum temperature to decrease gradually. The maximum temperature increased significantly when the amount of AHA was greater than 3% w/w of the dry mixture. Increasing the AHA content also improved the rate of the hydration reaction of the cement paste. Thus, AHA acted as an accelerator for cement mixtures. This result corresponded with the work by Chen and Sun (2018). When adding an amount of AHA greater than 3% w/w, however, the setting time is too rapid to form the fiber-cement product and the maximum temperatures are raised over 70 °C (Nithipaiboon et al., 2023). Therefore, the amount of 3% w/w AHA was selected to be added to the REF formula to enhance the early strength and shorten the setting time by approximately 40%.

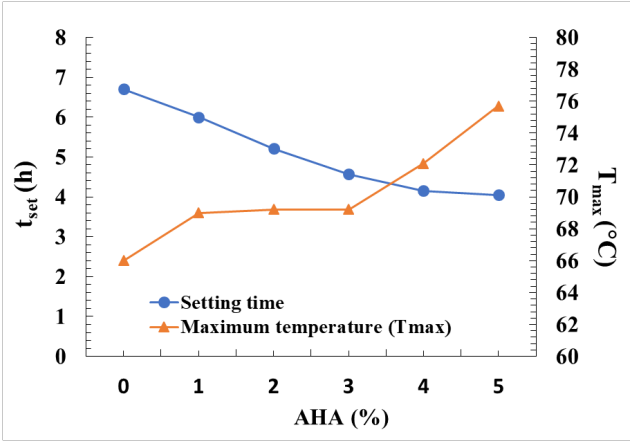


**Figure 1.** Relationship between the maximum temperature and setting time of cement paste versus AHA content

## 3.2 Phase analysis of fiber-cement composites by XRD and TGA

The effect of the AHA on the phase analysis of cement paste at curing days 7 and 28 is shown in Figure 2. The main hydration products during the curing of the cement paste are $Ca(OH)_2$, $CaCO_3$, AFt (Ettringite) and C-S-H. The intensity of diffraction peaks of $Ca(OH)_2$ ($2\theta \approx 18°$, 34°), $CaCO_3$ ($2\theta \approx 29°$) and ettringite ($2\theta \approx 41°$) increased significantly at an early age with 3% w/w AHA content, indicating that the AHA enhanced the hydration product of cement in the early stages, as in Figure 2(a). The intensity of the diffraction peaks of $C_3S$ ($2\theta \approx 32°$) decreased with increasing hydration age, as shown in Figure 2(b). This is to be expected as $C_3S$ is consumed to form C-S-H and the continuous hydration of calcium silicate phases (Chen and Sun, 2018; Mailar et al., 2016).

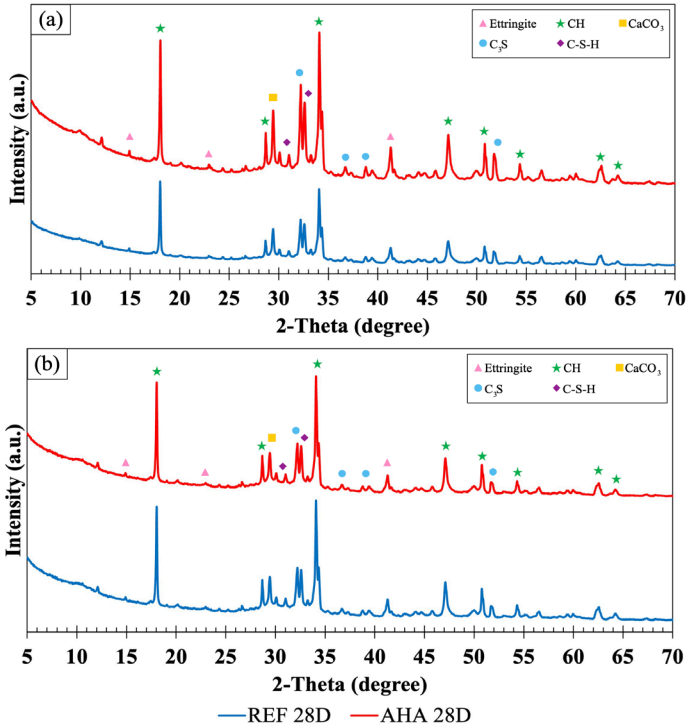


**Figure 2.** XRD pattern of fiber-cement composite samples; (a) air-cured for 7 days, and (b) 28 days

XRD data may not be sufficient to determine the hydration product of cement pastes. According to a report by Bhatty and Reid (1985), the temperature ranges for estimating the chemically bound water and the degree of hydration of the mixtures are between 100 and 1,000 °C. The three main endothermal peaks on DTG curves are the peaks of C-S-H and ettringite (100–400 °C), $Ca(OH)_2$ (400–600 °C), and $CaCO_3$ (600–1,000 °C), as shown in Figure 3 (Scrivener et al., 2016; Ou et al., 2011; Li et al., 2021; Liu et al., 2021). Weight loss of between 100 to 400 °C was caused by the dehydration of bound water from the C-S-H and ettringite ($L_{dh}$). Weight loss of around 400 to 600 °C was due to the dehydroxylation of $Ca(OH)_2$ ($L_{dx}$). Furthermore, between 600 to 1,000 °C, the weight loss was from the decarbonization reaction of $CaCO_3$ ($L_{dc}$). The mass loss and peak of C-S-H, ettringite, and $Ca(OH)_2$ from the TGA curves increased gradually with curing age. The chemically bound water ($W_B$) and the degree of hydration ($\propto$) of the mixtures were determined with the method of Bhatty and Reid (1985) using Equation (1) and (2), which are listed in Table 3.

$$W_B = L_{dh} + L_{dx} + 0.41\ (L_{dc}) \quad (1)$$

$$\propto = W_B\ /0.24 \quad (2)$$

The calculated hydration degree of the AHA cement paste increased rapidly in 14 days, compared to the REF formula, as shown in Figure 4. The degree of hydration for the AHA formula was found to be 58 and 61% at 14 and 28 days, respectively, which were higher than the REF formula. Thus, the addition of AHA significantly enhanced the hydration kinetics.

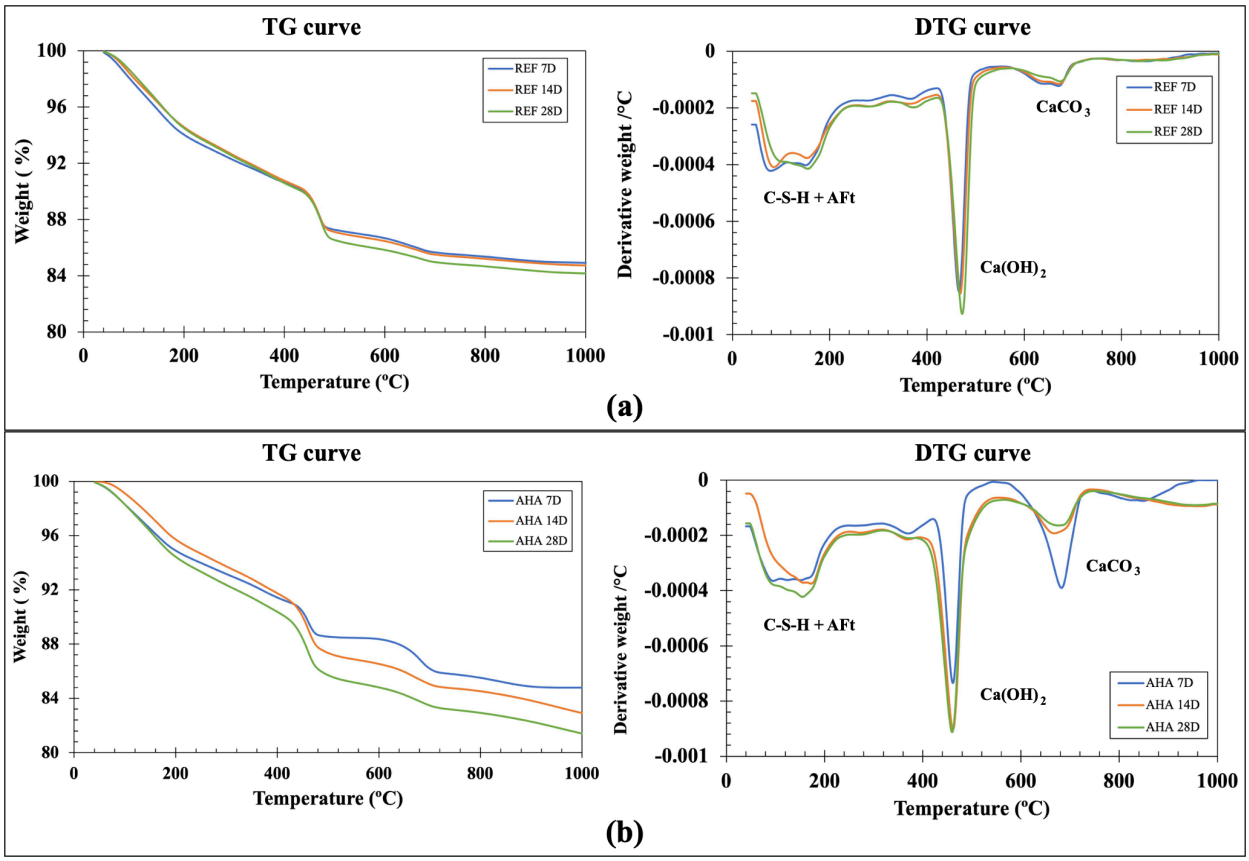


**Figure 3.** TG-DTG curves of fiber-cement composite samples; (a) REF, and (b) AHA air-cured for 7, 14 and 28 days

**Table 3.** Mass lost values and the values of $W_B$ and $\propto$ according to Equations (1) and (2)

| Mix | Age (days) | $M_{100\,°C}$ (%) | $M_{100\,°C}$ (%) | $M_{100\,°C}$ (%) | $M_{100\,°C}$ (%) | *Ldh* | *Ldh* | *Ldc* | $W_B$ | $\propto$ (%) |
|---|---|---|---|---|---|---|---|---|---|---|
| REF | 7 | 97.6835 | 90.6181 | 86.9765 | 84.9165 | 7.0654 | 3.6416 | 2.06 | 11.55 | 48.13 |
| | 14 | 98.0557 | 90.7584 | 86.7213 | 84.7358 | 7.2973 | 4.0371 | 1.9855 | 12.15 | 50.62 |
| | 28 | 98.2992 | 90.5897 | 86.1457 | 84.1695 | 7.7095 | 4.444 | 1.9762 | 12.96 | 54.01 |
| AHA | 7 | 98.2903 | 91.433 | 88.4604 | 84.7877 | 6.8573 | 2.9726 | 3.6727 | 11.34 | 47.23 |
| | 14 | 99.1101 | 91.7488 | 86.8832 | 82.9144 | 7.3613 | 4.8656 | 3.9688 | 13.85 | 57.72 |
| | 28 | 98.2846 | 90.3786 | 85.1829 | 81.4081 | 7.906 | 5.1957 | 3.7748 | 14.65 | 61.03 |

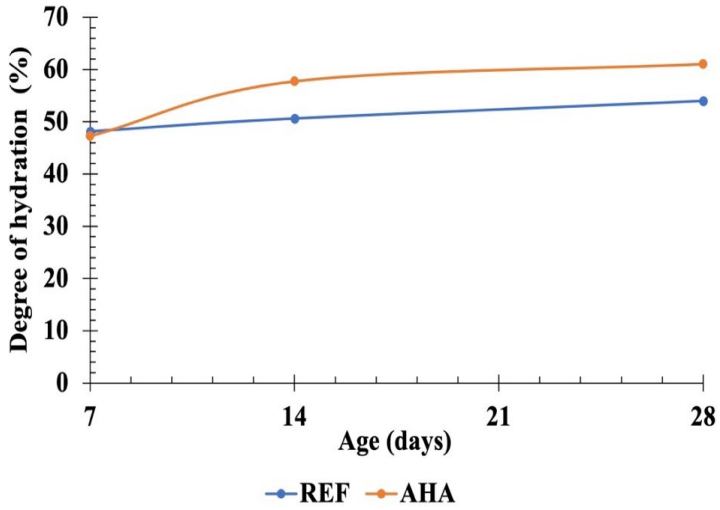


**Figure 4.** The hydration degree of cement pastes calculated using Bhatty's method (Bhatty and Reid, 1985)

### 3.3 Physical properties of fiber-cement composites

The effects of the AHA on the physical properties of fiber-cement composites cured for 7, 14 and 28 days are presented in Figures 5(a) and (b). The horizontal dash line indicates the minimum requirement for wallboard applications, according to the Thai Industrial Standards Institute provided in Table 4. The results showed no difference in bulk density for both the REF and the 3% w/w AHA formula. According to the Thai Industrial Standards Institute, the value of the required density for wallboard applications should be greater than 1.35 g/cc, and the water absorption must be lower than 25%. The results revealed that 3% w/w AHA can be used as an additive in fiber-cement composites and still meet these standards. Moreover, the results presented a significant decrease in water absorption in the samples prepared from 3% w/w AHA formula from 20% to less than 15%, compared to the REF formula.

The average modulus of elasticity (MOE), modulus of rupture (MOR), and impact strength data were obtained from the samples cured for 7, 14, and 28 days, as shown in Figure 6 (a) and (b). The mechanical properties of the composites still satisfy the requirement for wallboard applications provided in Table 4 (TISI, 2018). When AHA is added to the mixtures, early strength development such as MOE, MOR, and impact strength of the samples air cured for 7 days improved significantly.

**Table 4.** Required properties of fiber-cement for wallboard (Thai Industrial Standards Institute, 2018)

| Properties | MOR (MPa) | MOE (MPa) | Impact strength (J/m²) | Density (g/cc) | Water absorption (%) |
|---|---|---|---|---|---|
| Requirement | >7 | >5500 | >2500 | >1.35 | ≤ 25 |

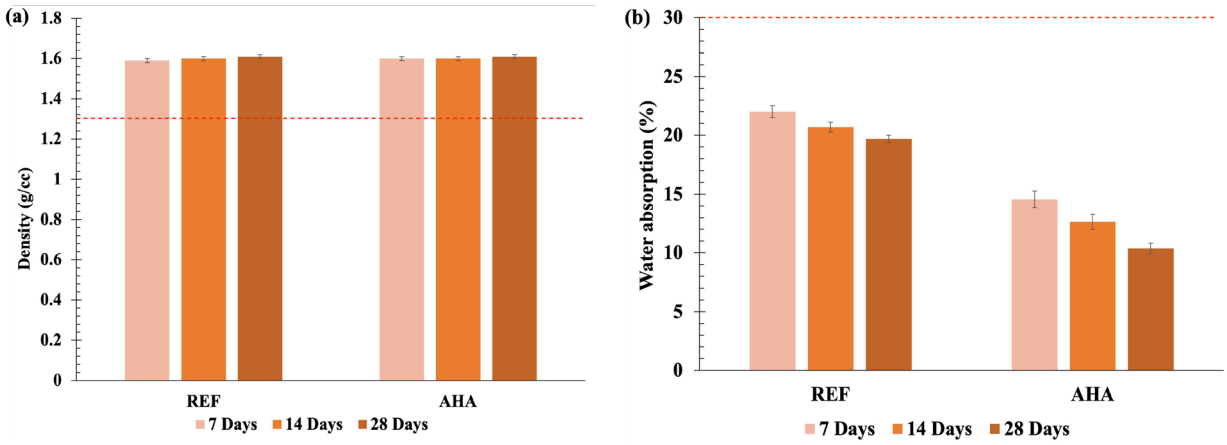


**Figure 5.** (a) Bulk density, and (b) water absorption of REF and 3% AHA samples air-cured for 7, 14 and 28 days
Note: The horizontal dash line indicates the minimum requirement for wallboard applications.

Compared to the REF control mixture, the MOE increased by 33% in the samples prepared with 3% w/w AHA mixture cured for 28 days. The MOR and impact strength results showed an average improvement of 22% and 16%, respectively, for the sample having a 3% w/w AHA mixture. According to a previous study by Elseknidy et al. (2020), a concrete mixture containing aluminum dross and quarry dust of more than 10 % and 20%, respectively, showed an increase in compressive and flexural strength, compared to the control mixture. Moreover, Salvador et al. (2016) reported that a small amount of aluminum-based additive containing $Al^{3+}$ further promoted the C-S-H gel by accelerating the hydration reaction of $C_3S$.

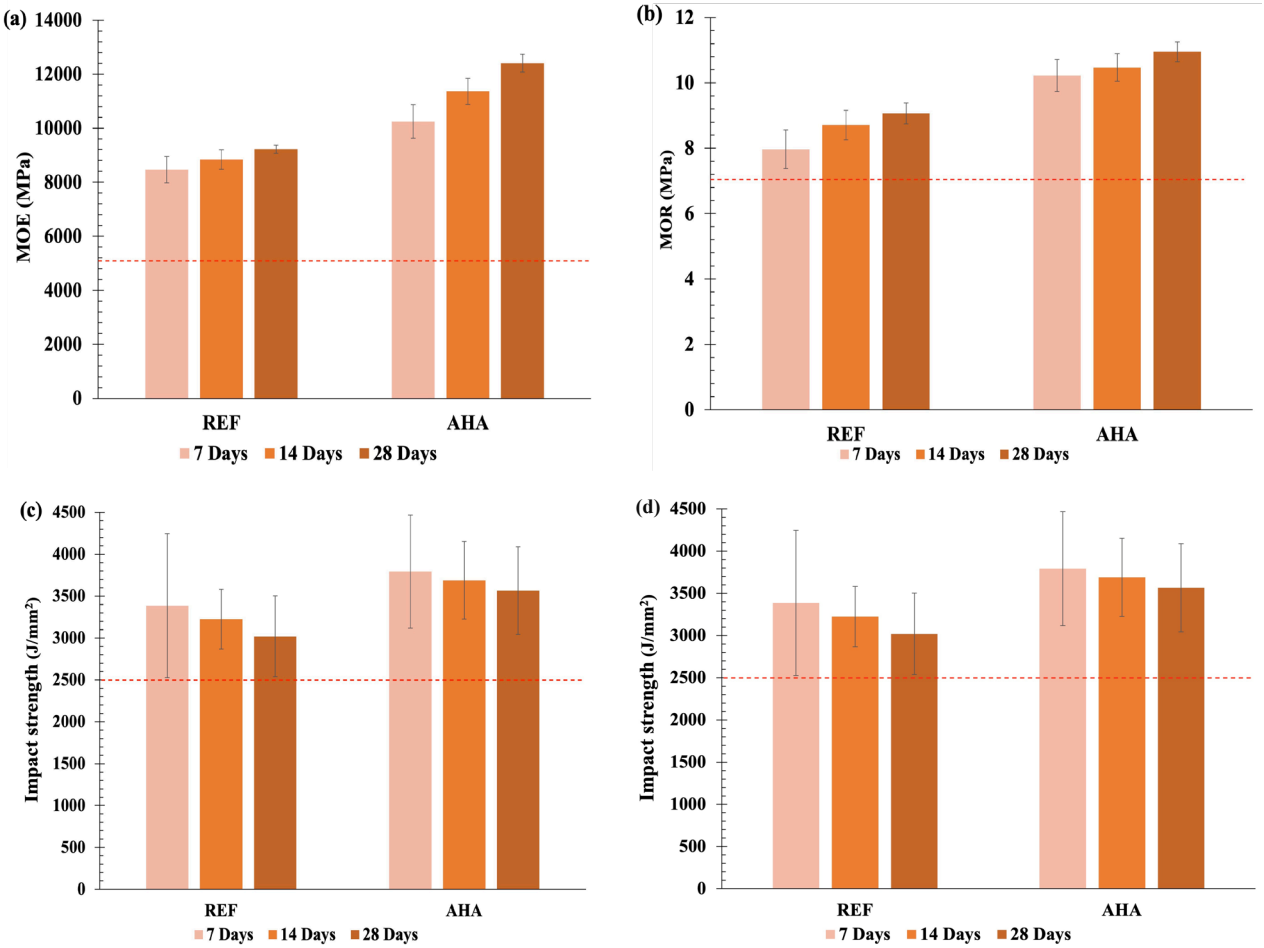


**Figure 6.** (a) MOE, (b) MOR and (c) impact strength of REF (d) and 3% w/w AHA samples air-cured for 7, 14 and 28 days
Note: The horizontal dash line indicates the minimum requirement for wallboard applications

The SEM micrographs in Figure 7 and Figure 8 show the microstructures of the cement matrix of the samples with and without the AHA. The micrographs showed that adding AHA changed the morphology of the crystalline phase. The microstructure of the REF sample showed a cotton-like structure of the C-S-H phase produced from the hydration reaction of OPC. By introducing AHA, more C-S-H and needle-shape ettringite phase (AFt) are present and fill in the typical pores. This corresponded to the increased hydration reaction and the heat evolution reported in Section 3.1. Increasing the AHA content enhanced the degree of hydration as well as the formation of needle-shape ettringite and C-S-H. In a previous study, Salvador et al. (2016) discovered that alkaline accelerators containing $Al^{3+}$ in their composition could react with $Ca^{2+}$ and $SO_4^{2-}$ in the high pH liquid phase of cement paste to rapidly form ettringite ($3CaOAl_2O_33CaSO_432H_2O$). In addition, the amount of the reinforcement phases affected the mechanical properties of the cement matrix (Chen and Sun, 2018). Thus, the addition of AHA promotes the formation of ettringite and improves the early strength of fiber-cement composites.

It has also been revealed that the addition of AHA can reduce the degree of water absorption of the samples due to small crystals in the cement matrix and the improvement of packing efficiency of the crystalline phase, as seen in Figure 8. This result also corresponds with previous work by Chakartnarodom et al. (2019). The use of an additive could change the morphology of the crystalline phase to the AFt phase in the cement matrix and cause reduced water absorption and enhanced mechanical properties, such as the MOE and MOR of the composites.

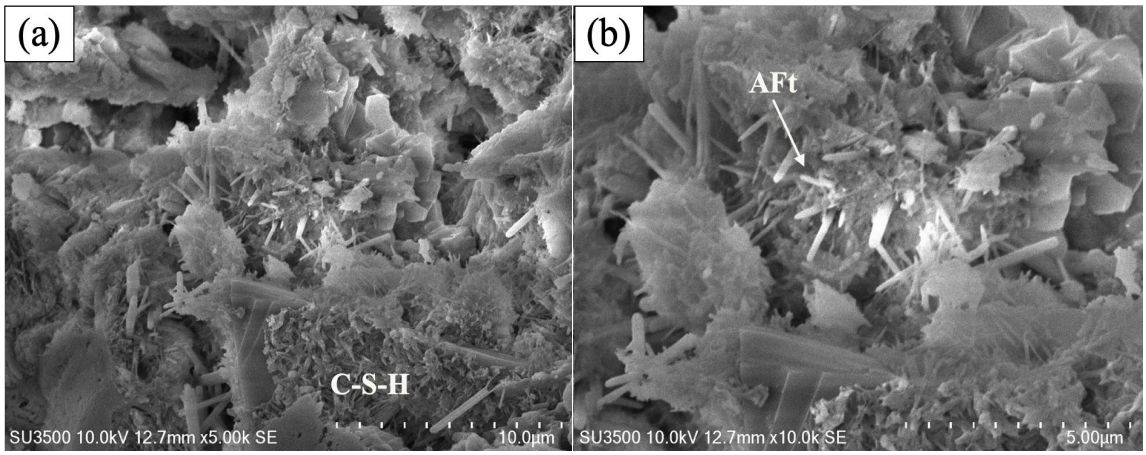


**Figure 7.** SEM micrographs at (a) 5000X and (b) 10000X, showing the microstructure of the REF sample

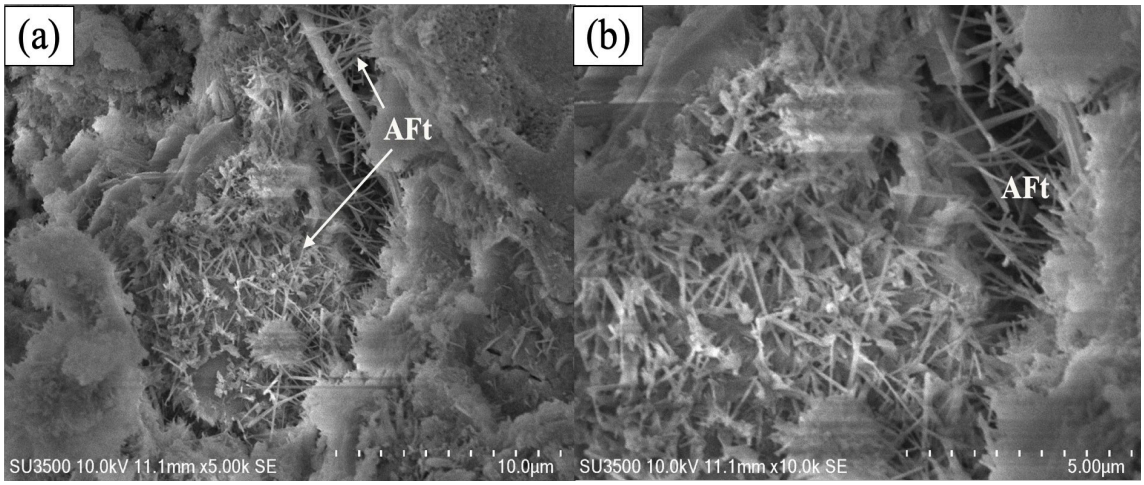


**Figure 8.** SEM micrographs at (a) 5000X and (b) 10000X, showing the microstructure of the sample that used 3% AHA

Pore structure analysis, characterizing pore parameters of the samples such as total porosity and volume-median pore size, are given in Table 5. The samples prepared from the AHA formula showed lower total porosity and volume-median pore size, compared to the REF formula. The results of the higher compactness of the samples containing AHA corresponded to lower water absorption and higher mechanical strength of fiber-cement composites.

**Table 5.** Characteristic pore parameters of the REF and 3% w/w AHA samples

| Sample | Porosity (%) | Volume-median pore size (μm) |
|---|---|---|
| **REF** | 24.09 | 43.57 |
| **AHA** | 16.51 | 7.59 |

The differential pore size distribution and cumulative intrusion of the samples cured for 28 days are plotted in Figure 9. The pores are classified into 4 groups including gel pores (<0.01μm), medium capillary pores (0.01–0.1 μm), large capillary (0.1–10 μm) and air voids (>10 μm) (Gomes and Savastano, 2014; Zhao et al., 2022; Long et al., 2021). From the MIP results, the volume of large pores (void pores), capillary pores, and gel pores decreases in the AHA sample. These observations and the formation and growth of hydration products in the pore space in the AHA sample resulted in a decrease in the volume of the total pores.

Images of the fiber-cement composite sample and the magnitudes of contact angle for water on the surface of REF and AHA samples cured for 28 days are shown in Figure 10. The hydrophilic nature of the surface of standard samples is shown in Figure 7(a), in which the contact angle is 45.3°. The surface of the AHA samples showed hydrophobic nature with a contact angle of 141.09°, as in Figure 7(b). These results confirm the addition of the AHA in fiber-cement composite reduces water absorption and improves the hydrophobicity of the composites.

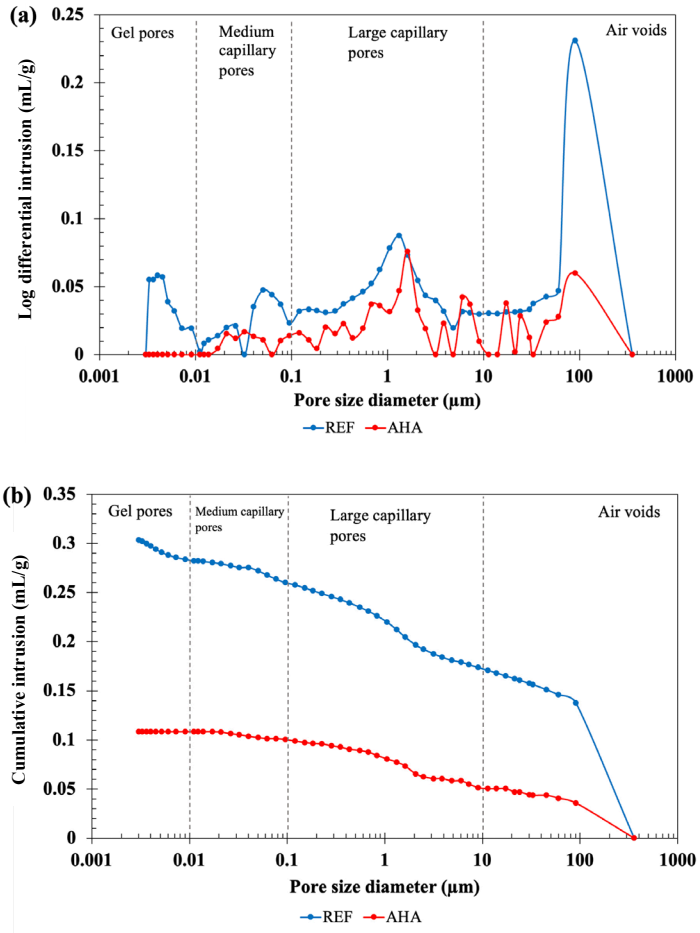


**Figure 9.** MIP analysis showing the microstructure of the REF and 3% AHA samples at day 28; (a) log differential intrusion, and (b) cumulative intrusion

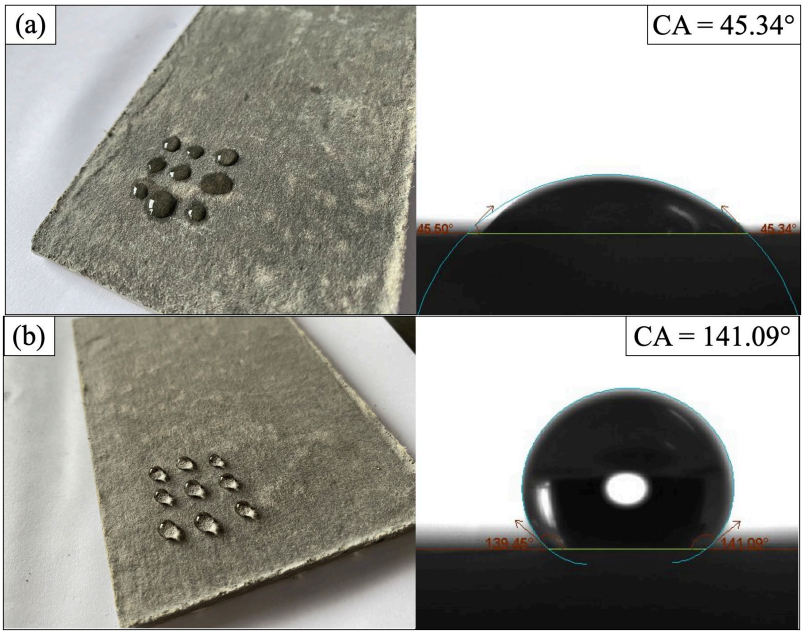


**Figure 10.** Images of water droplets on the sample surface of (a) REF sample, and the measurement result of the contact angle, and (b) AHA sample, and the measurement result of the contact angle cured for 28 days
Note: The contact angles were measured between the horizontal line of the specimen surface and the line tangent to the liquid droplet

## 4. CONCLUSION

The development of a hydrophobic fiber-reinforced cement composite by incorporating an AHA was examined. The results indicated that using 3% w/w of AHA in fiber-reinforced cement composites not only enhanced the heat of hydration but also led to a significant reduction in the setting time by approximately 40%. Moreover, the hydrophobic behavior, as evidenced by a contact angle of 141.09°, was achieved in the sample containing 3% w/w of AHA. The microstructure characteristics revealed that the AHA had a direct effect on the morphology of the cement hydration products, resulting in a reduction in crystalline size and the formation of a denser packing matrix. This close-packing microstructure caused a decrease in water absorption. The mechanical properties, especially the modulus of rupture and modulus of elasticity, were improved by the addition of the AHA. Analyses using MIP and thermogravimetry demonstrated improvements in the pore structure of cement and the degree of hydration due to the addition of the AHA.

## ACKNOWLEDGMENT

This work was supported by Shera Public Company Limited and the Faculty of Science and Technology, Thammasat University.

## REFERENCES

Abdalla, J. A., Thomas, B. S., Hawileh, R. A., Yang, J., Jindal, B. B., and Ariyachandra, E. (2022). Influence of nano-$TiO_2$, nano-$Fe_2O_3$, nanoclay and nano-$CaCO_3$ on the properties of cement/geopolymer concrete. *Cleaner Materials*, 4, 100061.

Azarhomayun, F., Haji, M., Kioumarsi, M., and Shekarchi, M. (2022). Effect of calcium stearate and aluminum powder on free and restrained drying shrinkage, crack characteristic and mechanical properties of concrete. *Cement and Concrete Composites*, 125, 104276.

Azarsa, P., Gupta, R., and Biparva, A. (2020). Inventive microstructural and durability investigation of cementitious composites involving crystalline waterproofing admixtures and Portland limestone cement. *Materials*, 13(6), 1425.

Bhatty, J. I., and Reid, K. J. (1985). Use of thermal analysis in the hydration studies of a type 1 Portland cement produced from mineral tailings. *Thermochimica Acta*, 91, 95–105.

Chakartnarodom, P., Kongkajun, N., Chuankrerkkul, N., Ineure, P., and Prakaypan, W. (2019). Reducing water absorption of fiber-cement composites for exterior applications by crystal modification method. *Journal of Metals, Materials and Minerals*, 29(4), 90–98.

Chen, C., and Sun, Z. (2018). Influence of aluminum sulfate on hydration and properties of cement pastes. *Journal of Advanced Concrete Technology*, 16(10), 522–530.

Chen, C.-Y., Shen, Z.-Y., and Lee, M.-T. (2021). On developing a hydrophobic rubberized cement paste. *Materials*, 14(13), 3687.

Elseknidy, M. H., Salmiaton, A., Shafizah, I. N, and Saad, A. H. (2020). A study on mechanical properties of concrete incorporating aluminum dross, fly ash, and quarry dust. *Sustainability*, 12(21), 9230.

Faraj, R. H., Mohammed, A. A., and Omer, K. M. (2022). Self-compacting concrete composites modified with nanoparticles: a comprehensive review, analysis and modeling. *Journal of Building Engineering*, 50, 104170.

Gomes, C. E. M., and Savastano, H., Jr,. (2014). Study of hygral behavior of non-asbestos fiber cement made by similar Hatschek process. *Materials Research*, 17(1), 121–129.

Khorami, M., and Ganjian, E. (2011). Comparing flexural behaviour of fibre-cement composites reinforced bagasse: wheat and eucalyptus. *Construction and Building Materials*, 25(9), 3661–3667.

Lagazzo, A., Vicini, S., Cattaneo, C., and Botter, R. (2016). Effect of fatty acid soap on microstructure of lime-cement mortar. *Construction and Building Materials*, 116, 384–390.

Li, C., Zhou, A., Zeng, J., Liu, Z., and Zhang, Z. (2019). Influence of MFPSA on mechanical and hydrophobic behaviour of fiber cement products. *Construction and Building Materials*, 223, 1016–1029.

Li, H., Xue, Z., Liang, G., Wu, K., Dong, B., and Wang, W. (2021). Effect of CS-Hs-PCE and sodium sulfate on the hydration kinetics and mechanical properties of cement paste. *Construction and Building Materials*, 266, 121096.

Li, R., Hou, P., Xie, N., Ye, Z., Cheng, X., and Shah, S. P. (2018). Design of $SiO_2$/PMHS hybrid nanocomposite for surface treatment of cement-based materials. *Cement and Concrete Composites*, 87, 89–97.

Liu, J., Janjua, Z. A., Roe, M., Xu, F., Turnbull, B., Choi, K.-S., and Hou, X. (2016). Super-hydrophobic/icephobic coatings based on silica nanoparticles modified by self-assembled monolayers. *Nanomaterials*, 6(12), 232.

Liu, P., Gao, Y., Wang, F., Yang, J., Yu, X., Zhang, W., and Yang, L. (2017). Superhydrophobic and self-cleaning behavior of Portland cement with lotus-leaf-like microstructure. *Journal of Cleaner Production*, 156, 775–785.

Liu, S., Shen, Y., Wang, Y., He, H., Luo, S., and Huang, C. (2021). Synergistic use of sodium bicarbonate and aluminum sulfate to enhance the hydration and hardening properties of Portland cement paste. *Construction and Building Materials*, 299, 124248.

Long, W.-J., Li, H.-D., Mei, L., Li, W., Xing, F., and Khayat, K. H. (2021). Damping characteristics of PVA fiber-reinforced cementitious composite containing high-volume fly ash under frequency-temperature coupling effects. *Cement and Concrete Composites*, 118, 103911.

Mailar, G., Raghavendra N, S., Sreedhara, B. M., Manu, D. S., Hiremath, P., and Jayakesh, K. (2016). Investigation of concrete produced using recycled aluminium dross for hot weather concreting conditions. *Resource-Efficient Technologies*, 2(2), 68–80.

Min, H., and Song, Z. (2018). Investigation on the sulfuric acid corrosion mechanism for concrete in soaking environment. *Advances in Materials Science and Engineering*, 2018, 3258123.

Mohr, B. J., Nanko, H., and Kurtis, K. E. (2005). Durability of kraft pulp fiber-cement composites to wet/dry cycling. *Cement and Concrete Composites*, 27(4), 435–448.

Nithipaiboon, J., Prakaypan, W., Chakartnarodom, P., Laitila, E. A., and Kongkajun, N. (2023). Impact of the hybrid-aluminum additive on the hydration kinetics of Portland cement in fiber-reinforced cement composites. *Suan Sunandha Science and Technology Journal*, 10(1), 126–131.

Ou, Z. H., Ma, B. G., and Jian, S. W. (2011). Comparison of FT-IR, thermal analysis and XRD for determination of products of cement hydration. *Advanced Materials Research*, 168–170, 518–522.

Pang, M., Sun, Z., and Huang, H. (2020). Compressive strength and durability of FGD gypsum-based mortars blended with ground granulated blast furnace slag. *Materials*, 13(15), 3383.

Raabe, J., Silva, D. W., Del Menezzi, C. H. S., and Tonoli, G. H. D. (2022). Impact of nanosilica deposited on cellulose pulp fibers surface on hydration and fiber-cement compressive strength. *Construction and Building Materials*, 326, 126847.

Sadrolodabaee, P., Claramunt, J., Ardanuy, M., and de la Fuente, A. (2021). Mechanical and durability characterization of a new textile waste micro-fiber reinforced cement composite for building applications. *Case Studies in Construction Materials*, 14, e00492.

Salvador, R. P., Cavalaro, S. H. P, Segura, I., Figueiredo, A. D., and Pérez, J. (2016). Early age hydration of cement pastes with alkaline and alkali-free accelerators for sprayed concrete. *Construction and Building Materials*, 111, 386–398.

Scrivener, K., Snellings, R., and Lothenbach, B. (2016). *A Practical Guide to Microstructural Analysis of Cementitious Materials (Vol. 540)*. Florida: CRC Press.

Thai Industrial Standards Institute (TISI). (2018). *Thai industrial standard TISI, subject: Fiber-cement sheets, no. 1427–2561*. Office of Product Standards Ministry of Industry. [in Thai]

Wong, H. S., Barakat, R., Alhilali, A., Saleh, M., and Cheeseman, C. R. (2015). Hydrophobic concrete using waste paper sludge ash. *Cement and Concrete Research*, 70, 9–20.

Yao, H., Xie, Z., Huang, C., Yuan, Q., and Yu, Z. (2021). Recent progress of hydrophobic cement-based materials: Preparation, characterization and properties. *Construction and Building Materials*, 299, 124255.

Zhao, B., Tan, Y., Yu, J., Xiao, H., Long, X., and Meng, J. (2022). Influence of Cementitious Capillary Crystalline Waterproofing Material on Mechanical Properties and Resistance to Chloride Ion Penetration of Engineered Cementitious Composites. *Social Science Research Network*, 4200011.

Zheng, K., Yang, X., Chen, R., and Xu, L. (2019). Application of a capillary crystalline material to enhance cement grout for sealing tunnel leakage. *Construction and Building Materials*, 214, 497–505.